Possibility of like-charged particles to attract each other at negative permittivity

Yakov M. Strelniker [1,*] and David J. Bergman[2,†]

[1]*Department of Physics, Bar-Ilan University, IL-52900 Ramat-Gan, Israel*

[2]*Raymond and Beverly Sackler School of Physics and Astronomy, Faculty of Exact Sciences, Tel Aviv University, IL-69978 Tel Aviv, Israel*

It is discussed whether like charges can be attracted to each other at a negative permittivity. The possibility of achieving negative permittivity in dielectric-conductor metamaterials due to localized surface plasmon resonance is shown. The possibility of manipulating the resonance frequency in a wide range of frequencies from zero to the plasma frequency by applying a magnetic or electric field is shown. The possibility of breakup of electron-hole pairs (exciton cold dissociation) and formation of electron-electron bound pairs at negative permittivity and nonzero frequency is discussed.

I. INTRODUCTION

It is well known that the permittivity ε of metals can reach negative values. However, only very recently this fact was widely used in theoretical and experimental studies of metamaterials. This brings to mind fantastic and unexpected optical properties [1–3]. The relation between the electric displacement **D** and the electric field **E**

$$\mathbf{D} = \varepsilon \cdot \mathbf{E}, \tag{1}$$

shows that at negative ε, the directions of **D** and **E** are opposite. It is worth noting that the permittivity ε appears also in the law of the electrostatic Coulomb interaction of charged particles q_1 and q_2 at a distance r:

$$\mathbf{F} = \frac{1}{\varepsilon} \frac{q_1 q_2}{r^3} \mathbf{r}. \tag{2}$$

There is no doubt that the Coulomb interaction can be reduced or even enhanced by changing ε in the positive region [4]. However, it follows logically from Eq. (2) that the force **F** should reverse its direction when ε is negative. Therefore, like charges should attract each other, while unlike charges should repel each other. The consequence of this can lead to unexpected physical properties and fantastic technical applications but it requires theoretical justification and experimental verification. Especially because the Coulomb interaction of Eq. (2) in media is verified only for positive values of the permittivity ε. Moreover, in most physics texts it is declared that the medium weakens the Coulomb interaction, i.e., that ε should be not only positive but also greater than 1. Although Coulomb's law and the superposition principle for electric fields in vacuum are completely equivalent to Maxwell's equations for electrostatics, it is not obvious that the permittivitiy in Eqs. (1) and (2) is the same. This is somewhat similar to the situation in mechanics where the inertial mass (**F** = $m\mathbf{a}$) and gravitational mass ($F = \gamma \frac{m_1 m_2}{r^2}$) are not obviously

the same and their identity was used to form the theory of general relativity. The appearance of the relative permittivity in the Coulomb law is usually explained phenomenologically as a result of the polarization of the medium. An attempt to derive the permittivity by an elementary calculation of lattice sums in the dipole approximation (see Appendix B) gives the result $\varepsilon = 1$, which shows the nontriviality of this issue, which requires further study.

The possibility to change repulsion of like charges to attraction is discussed very rarely in the literature. Nevertheless, when the current work was under preparation, we found several publications devoted to this problem. As far as we know, one of the first authors who pointed to the possibility of using negative permittivity to change repulsion to attraction was Ginzburg [5]. However, he mentioned this only in order to illustrate qualitatively the appearance of Cooper pairs in superconductors. In the article by Kirzhnits [6] (which was written at the request of Ginzburg) it was stated explicitly: "There exists, in principle, a class of substances within which the static interaction of the electrons has the character not of repulsion, as in vacuo, but of attraction." The latter prediction is probably already verified experimentally, at least partially. In a recent publication [7] the observation of attraction between electrons was reported in the system of bubble and stripe phases at negative permittivity.

We have also found several other publications about this problem [8–13] (we do not consider attraction of metal nanoparticles [14] in an electrolyte solution [15]). In addition, it is obvious that this problem can be extended to the case of ions and nuclei. For example, in Ref. [16] it was recently reported that ^{6}Li nuclei may be bound into Cooper-pair-like states [using a two-dimensional (2D) optical dipole trap]. We think that the time has now come to study intensively the above mentioned opportunities which give a negative permittivity. In this article, we discuss whether electrons can attract each other when the permittivity is negative (the spin dependence of this will be ignored for the sake of simplicity). As we will show, this can be realized not only in the static regime but also at nonzero frequency. Negative values of permittivity we propose to achieve due to the localized surface plasmon

*Contact author: strelnik@mail.biu.ac.il
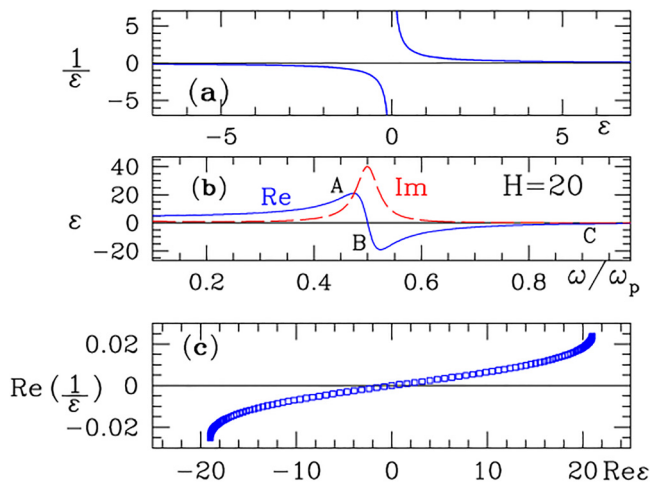†Contact author: bergman@tauex.tau.ac.il

FIG. 1. (a) Sketch of the $1/\varepsilon$ vs ε with discontinuity at the point $\varepsilon = 0$ when ε is assumed as real. (b) Real (blue solid line) and imaginary (red dashed line) parts of $\varepsilon \equiv \varepsilon_{xx}^{(M)}$ [given by Eq. (A1)] vs ω/ω_p for the dimensionless magnetic field $H = \omega_c \tau = 20$. $\omega_p \tau = 40$. (c) Real part of $1/\varepsilon$ vs. $Re\varepsilon$ when the existence of the imaginary part of ε is taken into account. The numerical values of ε are taken from the branch AB shown in (b).

FIG. 2. (a), (b) Similar to Figs. 1(b) and 1(c) but for the macroscopic dielectric permittivity ε_e of the conductor-insulator composite with conducting elliptical inclusions (shown in the inset). Results are obtained by Clausius-Mossotti (blue) and dilute (red) approximations (see Eqs. (15)–(18), (33) below and Refs. [18,19]) vs ω/ω_p. $\omega_p \tau = 40$. (b) The numerical values of ε_e are taken from the Clausius-Mossotti approximation branch AB shown in (a).

resonances (LSPR) in metamaterials. These resonance frequencies can be varied over a wide range by application of static magnetic or electric fields.

The remainder of this paper is organized as follows: In Sec. II we discuss the possibility to observe the attraction of like charges at a frequency in the range $0 < \omega < \omega_p$. In Sec. III we discuss the possibility of breakup of electron-hole pairs (dissociation of Wannier excitons) at negative permittivity and the creation of electron-electron or hole-hole pairs. In Sec. IV we present an analytical expression for LSPR in dielectric-conductor metamaterials and discuss the condition for achievement of negative permittivity ε. We conclude in Sec. V. In Appendix A we present an expression for the magnetic-field dependent permittivity tensor using the Drude approximation. In Appendices B and C we try to evaluate the relative dielectric constant of the Coulomb interaction in a classical approximation from first principles and show that it is equal to 1, i.e., that in the dipole approximation the medium does not affect the Coulomb interaction.

II. IMAGINARY PART OF THE PERMITTIVITY IN THE CASE OF ANOMALOUS DISPERSION

A. Imaginary part of ε

The work of Kirzhnits [6] was based mainly on the study of the Kramers-Kronig relations. Let us check here the possibility of zero and negative values of the relative permittivity ε in the Coulomb law from first principles. At first glance Eq. (2) should not be correct at negative values of ε since it has a discontinuity at $\varepsilon = 0$ as it is shown by the sketch in Fig. 1(a). However, it is known in the case of anomalous dispersion (namely, when it is possible to obtain zero or negative values of ε), the permittivity inevitably has an imaginary part [17]. In the case of normal dispersion, the imaginary part is usually small. Even from numerical calculations [see
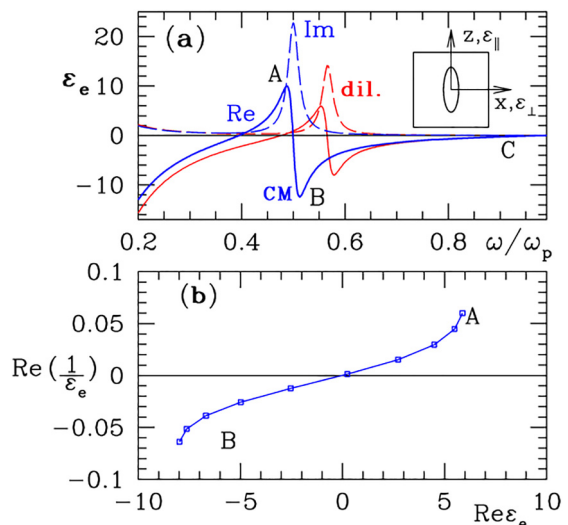
Fig. 1(b)] it follows that when the real part of ε vanishes, its imaginary part essentially differs from zero. These dependences are calculated using the Drude model of the metal permittivity tensor [see Eq. (A1) in the Appendix A]. The real part of the inverse permittivity, i.e., the value of $\mathrm{Re}(1/\varepsilon)$, passes continuously through zero, as shown in Fig. 1(c). This is obvious, since if the permittivity is complex $\varepsilon = \varepsilon' + i\varepsilon''$ then the inverse permittivity will also have a zero real part $\mathrm{Re}(1/\varepsilon) = \varepsilon'/(\varepsilon'^2 + \varepsilon''^2)$ when $\varepsilon' = 0$.

In Fig. 2 we show, similar to Fig. 1, dependences of the effective macroscopic permittivity ε_e and $\mathrm{Re}(1/\varepsilon_e)$ but obtained for a dielectric-conductor metamaterial. The results are obtained by using the dilute and Clausius-Mossotti approximations (see Eqs. (15)–(18), (33) below and Refs. [18,19]).

B. Non-Hermitian problem

The presence of the imaginary part of permittivity ε complicates the theory of considered phenomenon. In quantum mechanical description, the Hamiltonian in the Schrödinger equation will be non-Hermitian when the permittivity is complex. This also means that the solution will not be stationary and will be damped [20,21]. This can be seen directly from the time-dependent Schrödinger equation for a pair of quantum particles (see below) [22] $i\hbar \frac{\partial \psi}{\partial t} = (\frac{-\hbar^2 \nabla^2}{2\mu_{eh}} + V' - iV'')\psi$, where $\psi = \psi(\mathbf{r}, t)$ is the wave function, $V' - iV'' = e^2/[(\varepsilon' + i\varepsilon'')|\mathbf{r}|]$ is the complex Coulomb potential, $\mathbf{r}$ is the distance, $\hbar \equiv h/(2\pi)$ is Planck's constant, and μ_{eh} is the reduced mass of a pair of particles "e" and "h" (see below). Multiplying the above Schrödinger equation by ψ^* and the complex conjugated equation by ψ we get $\frac{\partial \rho}{\partial t} + \nabla \cdot \mathbf{J} = -\frac{V''}{\hbar}\rho$, where $\rho \equiv \psi^* \psi$ is the particle density and

$\mathbf{J} \equiv \frac{i\hbar}{2\mu_{\mathrm{eh}}}(\psi\nabla\psi^* - \psi^*\nabla\psi)$ is the current density. Therefore, in the steady state the particle density is attenuated by V''.

The influence of the imaginary part of the Coulomb potential can be illustrated also in the framework of Newton dynamics. The potential in Newton's second law (written along the x axis) $\ddot{x} + e^2/(\varepsilon\mu_{\mathrm{eh}}x^2) = 0$ can be expanded in series near the initial position R_0: $\frac{1}{(R_0-x)^2} \simeq \frac{1}{R_0^2} + \frac{2x}{R_0^3} + \frac{3x^2}{R_0^4} + \ldots$. Up to the term linear in x we have $\ddot{x} + \omega_0^2 x = -e^2/(\varepsilon\mu_{\mathrm{eh}}R_0^2)$, where $\omega_0^2 = \frac{\varepsilon'-i\varepsilon''}{\varepsilon'^2+\varepsilon''^2}\frac{2e^2}{\mu_{eh}R_0^3} = Ae^{i\phi}$, $A = \frac{2e^2}{\mu_{eh}R_0^3}(\frac{\varepsilon'}{\varepsilon'^2+\varepsilon''^2})$, $\phi = -\arctan(\frac{\varepsilon''}{\varepsilon'})$. The solution of this is

$$x = x_1 e^{\pm i\omega_0 t} - \frac{R_0}{2} = x_1 e^{\mp\sqrt{A}\sin\frac{\phi}{2}t}e^{\pm i\sqrt{A}\cos\frac{\phi}{2}t} - \frac{R_0}{2}, \quad (3)$$

where x_1 is the amplitude of the "oscillations". Thus, the imaginary part of the Coulomb potential (due to imaginary part of permittivity ε) leads (as in optics) to damping. Whether the imaginary part of the permittivity ε prevents or helps the pairing of particles requires additional consideration. Meanwhile, from Fig. 5(c) and Figs. 6(b) and 6(c) (see below) it can be seen that it is possible to find frequencies for which $\varepsilon' < 0$ and $\varepsilon'' \simeq 0$. For simplicity we consider everywhere below the case $\varepsilon'' \simeq 0$.

III. ELECTRON OSCILLATION AND WANNIER EXCITONS

Kirzhnits [6] and others [8–10] have considered the static situation when the permittivity should be taken at zero frequency. To achieve negative values of the permittivity ε at zero frequency $\omega = 0$ is a main difficulty in this problem. The static case corresponds to an attraction of particles strictly along a straight line. According to classical mechanics [23], this is possible only when their angular momentum M is strictly equal to zero. If M is nonzero, then the particles will move along elliptical trajectories and the fall of a particle to the center will be impossible within the framework of classical mechanics. Though to reach a negative value of ε in the static regime [i.e., $\varepsilon(0) < 0$] is possible in metamaterials by application of magnetic [18,19,24–33] or electric [34] fields (see Sec. IV below), it is more convenient to use for this purpose permittivity at nonzero frequency ω which can be realized in the case of oscillating or rotating charges. If, for example, the point charges are rotating one about the other (around a common center like in the case of the Wannier excitons [35–40]) then from outside it looks like oscillations of the dipole moment, i.e., oscillations of the electric field. In this case the permittivity ε, as a response of the surrounding media to the perturbation caused by charge oscillations, should be used at the frequency of these oscillations. One needs only to check whether the permittivity ε at these frequencies can reach negative values. The situation is similar to a problem in the theory of Wannier excitons: which ε should be used in the Coulomb interaction of a hole with an electron. As was shown in Refs. [35,41] and [42], when the radius of the exciton orbit (electron-hole pair) is small and therefore the frequency of rotation is large then the permittivity should be taken as $\varepsilon = 1$, since the valence electrons of the crystal cannot follow the rapid motion of the electron-hole pair. By contrast, when the
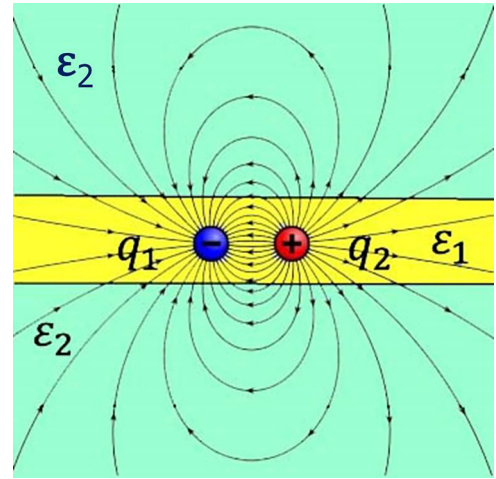

FIG. 3. Two point unlike charged q_1 and q_2 in a thin slab with permittivity ε_1 creating a bound electron-hole pair (exciton). Side view. Not all lines of the electrostatic forces are inside the slab. Therefore, the interaction between the point charges does not follow the Coulomb law [43–46]. The permittivity of the surrounding media is ε_2.

orbit radius is large the rotation frequency is small and the value of ε should be taken as the low frequency permittivity. As we will show in Sec. IV, negative values of ε can be achieved in the entire range of frequencies $0 < \omega < \omega_p$. That is, the frequency of exciton oscillation should be smaller than the plasma frequency ω_p (see Sec. IV and Appendix A).

The case of rotation of an electron around a hydrogen nucleus is often considered as a simple classical exercise. This can be treated as electric oscillations. From elementary evaluations ($m_e v^2/r_B = e^2/r_B^2$, where r_B is the Bohr radius, m_e is the electron mass), we can find the angular frequency of electron rotation $\omega_e = v/r = e/r_B^{3/2}m_e^{1/2} \simeq 4.1\times10^{16}$ rad/sec. Similarly, we can find the frequency ω_{ex} of rotation of electron and hole around their common center of mass in the case of the Wannier-Mott exciton [35–38] (i.e., a pair of electron and hole).

A. Modification of the Coulomb law in slabs: Method of images

We assume that the exciton is located in a thin dielectric slab (with positive permittivity $\varepsilon_1 > 0$) which is placed between two metal-dielectric media (with negative permittivity $\varepsilon_2 < 0$), see Fig. 3. Since not all lines of the electrostatic forces are inside the slab (see Fig. 3 and Refs. [43–46]) the interaction between the point charges does not follow the usual Coulomb law. Therefore the Coulomb interaction will depend not only on the permittivity ε_1 but also on ε_2. Therefore, when $\varepsilon_2 < 0$, the attraction between electron and hole can be changed to repulsion and the repulsion between electrons can be changed to attraction. This can be shown for example by the *method of images* [17,47]: In general this method is applied for the static case. However, if the relaxation time τ of electrons of the media with negative permittivity (see media with ε_2 in Figs. 3 and 4) is much less than the inverse frequency $1/\omega$ of the rotation (or oscillation) of the point charges ($-q_1$ and $-q_2$ in Fig. 4) in the media with ε_1 (i.e., $\tau << 1/\omega$), then the induced image charges in the medium with ε_2 ($+q_1'$ and
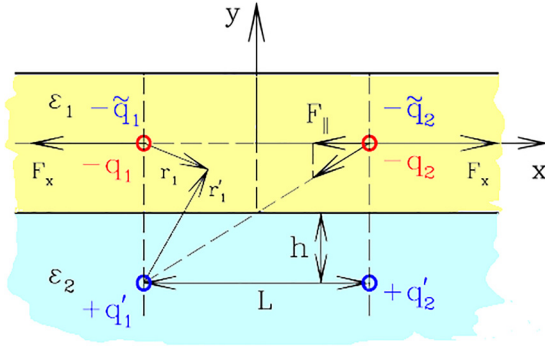
FIG. 4. Two point charges $-q_1$ and $-q_2$ in a slab with permittivity ε_1 above an infinitely thick medium with permittivity ε_2. The horizontal component of the Coulomb force $F_\parallel$ between charges $-q_1$ and $-q_2$ is calculated using the *method of images*.

$+q'_2$ in Fig. 4) will have time to form and the image method should work.

Similar to Ref. [10] we consider a system of two media: a dielectric slab with ε_1, placed on the top of the thick semiconductor slab with ε_2 (see Fig. 4). Above a dielectric slab with ε_1 it is possible to consider another thick slab with ε_2 like in Ref. [10], but we assume that this medium with ε_2 is a vacuum, what is easier to realize in experiment. Two point charges q_1 and q_2 ($q_1 = q_2$) are placed in a slab ε_1 at the distance L each from each other. The distance from the charges q_1 and q_2 to the lower medium ε_2 (and therefore from the induced charges q'_1 and q'_2 to the lower interface) is h. In the semiconductor due to the LSPR the negative permittivity $\varepsilon_2 < 0$ can be achieved, while in the dielectric $\varepsilon_1 \geqslant 1$. A point charge q_1 induces a point charge q'_1 in medium ε_2, while the point charge q'_1 induces in its turn a point charge $\tilde{q}_1$ in the medium ε_1 (see Fig. 4). Finally, it is possible to find [10,43–45] that the horizontal component of the Coulomb force acting on the point charge q_2 is equal (see Fig. 4):

$$F_\parallel = \frac{q_1 q_2}{\varepsilon_1 L^2} - \frac{2 q_2 q'_1 \cos \alpha}{\varepsilon_1 r^2}, \qquad (4)$$

where $r = \sqrt{L^2 + (2h)^2} = L/\cos \alpha$, $\tan \alpha = 2h/L$, $\cos \alpha = 1/\sqrt{1 + (2h)^2/L^2}$. Therefore,

$$F_\parallel = \frac{q_1 q_2}{\varepsilon_1 L^2} \left[1 - \frac{q'_1}{q_1} \cos^3 \alpha \right]$$

$$= \frac{q_1 q_2}{\varepsilon_1 L^2} \left[1 - \frac{\varepsilon_1 - \varepsilon_2}{\varepsilon_1 + \varepsilon_2} \frac{1}{\left(1 + \frac{4h^2}{L^2}\right)^{3/2}} \right]. \qquad (5)$$

When $4h^2/L^2 \ll 1$, Eq. (5) simplifies to the form

$$F_\parallel \approx \frac{q_1 q_2}{\varepsilon_1 L^2} \frac{2\varepsilon_2}{\varepsilon_2 + \varepsilon_1}. \qquad (6)$$

From Eq. (6) it follows that the like charges can attract each other when $\varepsilon_2 < 0$ while $\varepsilon_1 + \varepsilon_2 > 0$. Also the charges with different sign will then repel each other.

B. Excitonlike electron-electron bound pairs

According to Ref. [35], a pair of unlike charged electron and hole, i.e., a Wannier exciton of large radius, can be

roughly imagined if we consider only one excited electron and one hole in a crystal, and take into account the remaining emitted electrons and atomic cores by introducing a periodic potential that determines only the isotropic masses of an electron and a hole, etc. If we further assume that an electron and a hole in such a medium interact according to the Coulomb law ($-e^2/\varepsilon r_{eh}$), then the Schrödinger equation for the electron-hole system will have the following form:

$$\left(-\frac{\hbar^2 \nabla_e^2}{2m_e} - \frac{\hbar^2 \nabla_h^2}{2m_h} - \frac{e^2}{\varepsilon r_{eh}} \right) \Psi = E \Psi, \qquad (7)$$

where r_{eh} is the distance between the electron and the hole, Ψ is the wave function, and m_e and m_h are the electron and hole masses, respectively. This equation is written in the so-called effective mass approximation and is similar to the equation for the hydrogen atom [48]. The quantum-mechanical expression for the effective Bohr exciton radius [35–38] is

$$r_{ex} = \frac{\varepsilon \hbar^2}{e^2 \mu_{eh}}, \qquad (8)$$

where $\mu_{eh} = m_e m_h / (m_e + m_h)$ is the reduced mass of the exciton. This differs from the hydrogen Bohr radius [48] by the presence of the permittivity ε in the numerator. In semiconductors the typical permittivity ε is of order $\varepsilon \simeq 10$ and, therefore, the rotation frequency of the electron-hole pair is of order $\omega_{ex} \simeq 1.3 \times 10^{15}$ sec^{-1}, which is smaller than ω_e. This can be compared with the quantum estimation $\omega_{ex} =$ (angular momentum)/(mass $\cdot$ radius^2) (see Ref. [35]):

$$\omega_{ex} = \hbar / \mu_{eh} r^2. \qquad (9)$$

For an exciton with an effective mass $\mu_{eh} = m_e/2$ in a crystal with gap energy $E_G = 2$ eV and radius $r = 5$ Bohr radii we get $\omega_{ex} \approx 3 \times 10^{15}$ sec^{-1}, which is close to the previous classical estimation.

The linear velocity of the electron in an exciton can be estimated by $v = r_{ex} \omega_{ex} = \frac{\varepsilon_{ex} \hbar^2}{e^2 \mu_{eh}} \omega_{ex} \approx 1.4 \times 10^5$ m/sec. This is much less than one percent of the light speed 3×10^8 m/sec. Therefore the above classical estimates are reasonable.

We need to check whether the values of ω used above $\omega_{ex} \approx 1.3 \times 10^{15}$ sec^{-1} or $\omega_{ex} \approx 3 \times 10^{15}$ sec^{-1} are smaller than the plasma frequency ω_p:

$$\omega_p = \sqrt{\frac{4\pi N_0 e^2}{m_e}} = 5.64 \times 10^4 \sqrt{N_0} \text{ rad/sec}, \qquad (10)$$

where N_0 is the concentration of free electrons in the metal. Since for typical metals such as aluminum or silver N_0 is approximately 10^{23} cm^{-3}, the plasma frequency of Eq. (10) is of order $\omega_p \simeq 1.5 \times 10^{16}$ sec^{-1} (which is in the ultraviolet region). At the frequencies $\omega > \omega_p$ the metal permittivity $\varepsilon_m \simeq 1$ since the electrons of the surrounding media are unable to follow the electric field oscillations.

Since the frequency of the exciton oscillations ω_{ex} is much smaller than the plasma frequency ω_p, the permittivity ε in Eq. (8) can be differ from 1. By tuning the LSPR with an applied magnetic field [18,24–27,29–31] or an applied gate voltage [34], the permittivity ε_2 can be made negative at the frequency ω_{ex} (see Sec. IV below). Since the interaction between two point charges in a thin dielectric film with ε_1

depends also on the permittivity of a conducting film with ε_2, this should lead to breakup of electron-hole pairs (cold electrostatic exciton *dissociation*) and *creation* of electron-electron pairs (similar to Cooper pairs). Since the masses of the electron and the hole can be different, the exciton hydrogenic Rydberg constant $R_{\text{ex}} = \mu e^4/2\hbar^2\varepsilon_{\text{ex}}^2$ (see Ref. [35]) for the electron-hole pairs and the electro-electron pairs can also be different and the process of exciton destruction and creation of electron-electron pairs can be experimentally observable directly in the optical spectra of the same sample.

The electron-electron system with negative permittivity ε is also similar to positronium [49], but without annihilation. Two electrons can form a bound state but cannot enter into a fusion reaction since between electrons acts only the weak interaction but not the strong one as in the case of protons.

Another interesting phenomenon which can appear at negative permittivity $\varepsilon_e < 0$, and which should be discussed separately, is the ionization of atoms which is a consequence of repulsion of the atomic nucleus and its electron shell.

C. Nuclei-nuclei bound pairs

Whether it possible to obtain a nucleon-nucleon pairing at negative permittivity $\varepsilon < 0$ is an even more important question than the electron-electron pairing discussed above. Being substituted by a proton mass (instead an electron mass) into expression for Bohr radius it gives a value of order 3×10^{-14} m (when $|\varepsilon| = 1$), which is close to the distance $\sim 10^{-15}$ m, where the strong forces begin to act. That is, this estimation is very promising for reaching nuclear fusion. However, the other parameters (like rotation frequency and linear velocity of nuclei) obtained using the discussed above formulas are not realistic. Therefore, in contrast to the case of an electron-electron pair, such estimations for nuclei should be performed using relativistic quantum mechanics or other suitable approaches.

IV. ANALYTICAL AND NUMERICAL FORMALISM—RESONANCES

The negative permittivity ε needed for achieving attraction of like charges can be obtained in insulator-conductor metamaterials with appropriate nanostructures. The frequencies at which negative values of ε are achieved can be manipulated by an applied static magnetic [19,24–31] field **B** or electric gate voltage [34]. The theory and formalism of this are presented briefly below (taking into account all parameters in general form in order to find the best way for manipulating the resonant frequency and striving for its minimal values of frequency). We used a quasistatic approximation in which the wave vector $\mathbf{k} = 0$, i.e., the wavelength should be greater than the characteristic sizes of the nanostructures of the metamaterials. This approximation is used in many situations. The description of the more general case when $|\mathbf{k}| > 0$ can be found, e.g., in Refs. [4,50].

We consider a two-constituent insulator-conductor composite medium made of two uniform materials with permittivity tensors $\hat{\varepsilon}_1$ and $\hat{\varepsilon}_2$. The position-dependent local permittivity tensors $\hat{\varepsilon}(\mathbf{r})$ of this medium can be written as

$$\hat{\varepsilon} = \hat{\varepsilon}_1\theta_1 + \hat{\varepsilon}_2\theta_2 = \hat{\varepsilon}_2 - \delta\hat{\varepsilon}\theta_1, \qquad (11)$$

where $\delta\hat{\varepsilon} \equiv \hat{\varepsilon}_2 - \hat{\varepsilon}_1, \theta_2 = 1 - \theta_1$. Here we have used the characteristic or indicator function of the i constituent

$$\theta_i(\mathbf{r}) = \begin{cases} 1 & \text{for } \mathbf{r} \text{ inside the } i \text{ constituent,} \\ 0 & \text{elsewhere.} \end{cases} \qquad (12)$$

If the inclusions form a periodic lattice, this description is suitable, provided the lattice constant is much smaller than the wavelength, i.e., when the sample is homogeneous on the scale of the electromagnetic wavelength. Following our previous works [19,24–31,34], we choose a scheme where the composite medium occupies the entire volume in between the infinitely conducting plates of a parallel plate capacitor. The plates are taken to be infinitely large, and the distance between them is taken to be finite but large compared to any scale of inhomogeneity of the system. Keeping the medium fixed, we can choose the orientation of the plates to be perpendicular to any of the coordinate axes. We denote by $\phi^{(\alpha)}$ the local potential field that results when the plates are perpendicular to the r_α axis and a potential difference equal to their distance apart is applied between them. The volume averaged electric field is then $\langle\nabla\phi^{(\alpha)}\rangle = \nabla r_\alpha = \mathbf{e}_\alpha$, i.e., a unit vector in the r_α direction. The potential field $\phi^{(\alpha)}$ is the solution of the partial differential equation for the electric displacement $\nabla \cdot \mathbf{D} = \nabla \cdot \hat{\varepsilon}(\mathbf{r}) \cdot \phi^{(\alpha)}(\mathbf{r}) = 0$, namely

$$\nabla \cdot \hat{\varepsilon}_2 \cdot \nabla\phi^{(\alpha)} = \nabla \cdot \theta_1\delta\hat{\varepsilon} \cdot \nabla\phi^{(\alpha)}, \qquad (13)$$

and the boundary condition $\phi^{(\alpha)} = r_\alpha$ at the capacitor plates.

The bulk effective electric permittivity tensor is defined by

$$\hat{\varepsilon}^{(e)} \cdot \langle\mathbf{E}(\mathbf{r})\rangle \equiv \langle\hat{\varepsilon}(\mathbf{r}) \cdot \mathbf{E}(\mathbf{r})\rangle, \qquad (14)$$

where the angular brackets denote a volume average $\langle\ldots\rangle \equiv \frac{1}{V}\int dV\ldots$.

The case of a single inclusion of ellipsoidal or cylindrical shape can be solved exactly when $H \equiv \omega_c\tau = 0$. [47] Extensions of that solution for the case $H \neq 0$ were described in Refs. [19,24–29]. For a *dilute* system it immediately follows that

$$\hat{\varepsilon}^{(e)} = \hat{\varepsilon}_2 - p_1\delta\hat{\varepsilon} \cdot \hat{\gamma}, \qquad (15)$$

where $p_1 = V_{\text{inc}}/V$ is the volume fraction of the inclusions. When $\mathbf{B} \parallel z$ (i.e., when $\delta\varepsilon_{xz} = \delta\varepsilon_{yz} = \delta\varepsilon_{zx} = \delta\varepsilon_{zy} = 0$) the matrix $\hat{\gamma}$ takes the form [18,31]

$$\hat{\gamma} = \begin{pmatrix} \frac{1}{D}\left(1 - \frac{n_y\delta\varepsilon_{yy}}{\varepsilon_{yy}}\right) & \frac{1}{D}\frac{n_x\delta\varepsilon_{xy}}{\varepsilon_{yy}} & 0 \\ \frac{1}{D}\frac{n_y\delta\varepsilon_{yx}}{\varepsilon_{yy}} & \frac{1}{D}\left(1 - \frac{n_x\delta\varepsilon_{xx}}{\varepsilon_{xx}}\right) & 0 \\ 0 & 0 & \frac{1}{1-\frac{n_z\delta\varepsilon_{zz}}{\varepsilon_{zz}}} \end{pmatrix}, \qquad (16)$$

$$D = \left(1 - \frac{n_x\delta\varepsilon_{xx}}{\varepsilon_{xx}}\right)\left(1 - \frac{n_y\delta\varepsilon_{yy}}{\varepsilon_{yy}}\right) - n_xn_y\frac{\delta\varepsilon_{xy}}{\varepsilon_{xx}}\frac{\delta\varepsilon_{yx}}{\varepsilon_{yy}}, \qquad (17)$$

where n_x, n_y, and n_z are the depolarization factors [47] of the inclusion. Here we omit for simplicity the subscripts "2" in the host permittivity tensors $\hat{\varepsilon}_2$.

A. Insulating host and conducting ellipsoidal inclusions

Let us consider the case of insulating host and dilute conducting ellipsoidal inclusions. From Eqs. (15)–(17) we can write, for example, an expression for the xx-component of the permittivity tensor $\hat{\varepsilon}_e$:

$$\varepsilon_{xx}^{(e)} = \varepsilon_{xx}\left\{ 1 - p_1 \frac{(\varepsilon_{xx} - \varepsilon_{xx}^{(inc)})[\varepsilon_{yy} - n_y(\varepsilon_{yy} - \varepsilon_{yy}^{(inc)})] + \varepsilon_{xy}^{(inc)}\varepsilon_{yx}^{(inc)}n_y}{(\varepsilon_{xx} - n_x\delta\varepsilon_{xx})(\varepsilon_{yy} - n_y\delta\varepsilon_{yy}) - n_x n_y \delta\varepsilon_{xy}\delta\varepsilon_{yx}} \right\}, \tag{18}$$

where the host is insulator with ε_{xx}, ε_{yy}, and ε_{zz} permittivity tensor components (the off-diagonal components $\varepsilon_{xy} = \varepsilon_{xz} = \varepsilon_{yx} = \varepsilon_{zx} = 0$ vanish), while the permittivity tensor components of the conducting inclusions we indicate with superscript "inc" and take from Eq. (A1) (see below) in the limit $\omega\tau \gg 1$: $\varepsilon_{xx}^{(inc)} = \varepsilon_{yy}^{(inc)} = \varepsilon_0 - \frac{\omega_p^2}{\omega^2 - \omega_c^2}$, $\varepsilon_{xy}^{(inc)} = -\varepsilon_{yx}^{(inc)} = \frac{i\omega_p^2\omega_c}{\omega(\omega^2 - \omega_c^2)}$.

The determinant $D(\omega)$ in Eqs. (16) and (17) plays a crucial role when it is equal to zero and gives the values of the resonance frequencies. Substituting Eq. (A1) in the limit $\omega\tau \gg 1$ into Eq. (17) and equating it to zero, we get an equation for the resonance frequency ω_{res}. This condition can be rewritten as

$$\omega_{res}^2[\alpha(\omega_{res}^2 - \omega_c^2) - n_x\omega_p^2][\beta(\omega_{res}^2 - \omega_c^2) - n_y\omega_p^2]$$
$$= n_x n_y \omega_p^4 \omega_c^2, \tag{19}$$

where we have introduced the definitions $\alpha \equiv (1 - n_x)\varepsilon_{xx} + \varepsilon_0 n_x$ and $\beta \equiv (1 - n_y)\varepsilon_{yy} + \varepsilon_0 n_y$, and where ε_0 is the dielectric constant of the background ionic lattice [see Eq. (A1)]. This can be simplified to the form of a biquartic equation

$$(\omega_{res}^2 - \omega_c^2)\left[\omega_{res}^4 - (g\omega_p^2 + \omega_c^2)\omega_{res}^2 + \frac{n_x n_y \omega_p^4}{\alpha\beta}\right] = 0, \tag{20}$$

$$\text{where } g = \frac{n_x\beta + n_y\alpha}{\alpha\beta} = \frac{n_x}{\alpha} + \frac{n_y}{\beta}. \tag{21}$$

The solutions of Eq. (20) are

$$\omega_{res} = \pm\omega_c, \tag{22}$$

$$\omega_{res\pm}^2 = \frac{g\omega_p^2 + \omega_c^2}{2} \pm \sqrt{\frac{(g\omega_p^2 + \omega_c^2)^2}{4} - \frac{n_x n_y \omega_p^4}{\alpha\beta}}. \tag{23}$$

The resonance (22) is called the "cyclotron resonance". From Eq. (23) for $H = 0$ we immediately obtain the frequency $\omega_{res} = \omega_p\sqrt{n_x}$, which is known as the LSPR. However, as soon as $H > 0$, this splits into two resonances: a "magneto-plasma resonance" (denoted by ω_-) and a "magneto-plasma shifted cyclotron resonance" (denoted by ω_+) [19,24–30]. Equation (23) can be expanded in the limits $\omega_c/\omega_p \ll 1$ and $\omega_p/\omega_c \ll 1$. For a weak magnetic field (i.e., for $\omega_p \gg \omega_c$) we get

$$\omega_{res\pm} \simeq \left[\frac{g}{2} + \sqrt{\frac{g^2}{4} - \frac{n_x n_y}{\alpha\beta}}\right.$$
$$\left. + \frac{1}{4\sqrt{\frac{g}{2} \pm \sqrt{\frac{g^2}{4} - \frac{n_x n_y}{\alpha\beta}}}}\left(1 + \frac{g}{2\sqrt{\frac{g^2}{4} - \frac{n_x n_y}{\alpha\beta}}}\right)\left(\frac{\omega_c}{\omega_p}\right)^2\right]. \tag{24}$$

For a strong magnetic field (i.e., $\omega_c \gg \omega_p$) we get

$$\omega_{res+} \simeq \omega_c + \frac{g}{2}\frac{\omega_p^2}{\omega_c}, \tag{25}$$

$$\text{and } \omega_{res-} \simeq \sqrt{\frac{n_x n_y}{\alpha\beta}}\frac{\omega_p^2}{\omega_c}. \tag{26}$$

When

$$n_x = n_y \equiv n \text{ and } \varepsilon_{xx} = \varepsilon_{yy} = \varepsilon_0, \tag{27}$$

it then follows from Eqs. (25) and (26) that

$$\omega_{res+} \simeq \frac{n}{\varepsilon_0}\frac{\omega_p^2}{\omega_c} + \omega_c, \tag{28}$$

$$\omega_{res-} \simeq \frac{n}{\varepsilon_0}\frac{\omega_p^2}{\omega_c} \tag{29}$$

(note that for the sphere $n_x = n_y = n_z \equiv n = 1/3$). The situation with Eq. (24) is more complicated under the conditions (27) since for these parameters $\frac{g^2}{4} - \frac{n_x n_y}{\alpha\beta}$ vanishes. One needs to put conditions (27) into Eqs. (20) and (21), then these resonances take simple forms:

$$\omega_{res\pm} = \omega_p\sqrt{\frac{n}{\varepsilon_0} + \frac{1}{2}\left(\frac{\omega_c}{\omega_p}\right)^2 \pm \left(\frac{\omega_c}{\omega_p}\right)\sqrt{\frac{n}{\varepsilon_0} + \frac{1}{4}\left(\frac{\omega_c}{\omega_p}\right)^2}}. \tag{30}$$

From this we get an approximate expression in the limit $\omega_c \ll \omega_p$:

$$\omega_{res\pm} \simeq \omega_p\sqrt{\frac{n}{\varepsilon_0}} \pm \frac{\omega_c}{2} + \frac{1}{8}\sqrt{\frac{\varepsilon_0}{n}}\frac{\omega_c^2}{\omega_p}. \tag{31}$$

In order to observe the resonances (28), (29), and (31), the conductivity relaxation time τ must satisfy $\omega\tau > 1$. Such resonances were studied both experimentally and theoretically many years ago [51,52] as well as more recently [18,19,24–30] in the case of metamaterials.

When the applied magnetic field vanishes ($\omega_c = 0$), the expression for the resonance frequency follows directly from Eq. (30)

$$\omega_{res\pm} \simeq \omega_p\sqrt{\frac{n}{\varepsilon_0}}. \tag{32}$$

The expression for ω_{res} in the Clausius-Mossotti approximation has a similar form, one only needs to make the substitution [19] $n_i \to (1 - p_1)n_i$:

$$\omega_{res\pm} \simeq \omega_p\sqrt{\frac{(1 - p_1)n}{\varepsilon_0}}. \tag{33}$$

B. Cylindrical inclusions

When the cylinder axis is along the y axis then the depolarization factor in this direction is zero: $n_y = 0$. When the magnetic field is directed parallel to the z-axis, $\mathbf{B} \parallel z$, Eq. (16) simplifies and there are resonances when the denominator $D(\omega) = \varepsilon_{xx} - n_x \delta\varepsilon_{xx}$, or $D(\omega) = \varepsilon_{zz} - n_z \delta\varepsilon_{zz}$ vanishes.

When the elliptical cylinders are conducting and the host is insulating, the expression for the resonance frequency can be obtained directly from Eq. (23) just by putting $n_y = 0$:

$$\omega_{\text{res}} = \sqrt{\frac{n_x \omega_p^2}{(1 - n_x)\varepsilon_{xx} + \varepsilon_0 n_x} + \omega_c^2}. \quad (34)$$

We see that the value of ω_{res} only increases with the application of a magnetic field ω_c. However, ω_{res} can be decreased by decreasing the depolarization factor n_x from 0.5 to 0 and by increasing ε_0.

The case of insulating cylinders inside a conducting host at nonzero magnetic field H is more complicated and is discussed in Refs. [19,24–30].

C. Results

In Fig. 5 we show numerically calculated real (solid blue line) and imaginary (dashed red line) parts of $\varepsilon_{xx}^{(e)}$ of a periodic array of conducting spheres (of radii $R = 0.45a$, where a is the distance between the centers of neighboring spheres) vs dimensionless frequency ω/ω_p. The LSPR should appear at the frequency given by Eq. (33). However, there are essential shifts from these values due to large sphere radii when the dilute or Clausius-Mossotti approximation do not give good quantitative agreement. Larger values of the radii lead to deeper negative values of $\varepsilon_{xx}^{(e)}$ at the resonances in all cases of Fig. 5. In Fig. 5(a) we show the case of zero magnetic field $H = 0$. The LSPR should appear at the frequency $\omega_{\text{res}}/\omega_p \simeq 0.45$ [see Eq. (33)]. In the numerical calculation this resonance is shifted to lower frequencies due to large sphere radius $R = 0.45a$. Changing ε_0 [see Eq. (A1)] to the value $\varepsilon_0 = 10$ shifts the resonance by $\Delta\omega_3$ to the lower frequency $\omega_{\text{res}}/\omega_p \simeq 0.17$. Application of an external magnetic field $H = \omega_c \tau = \mu_e |\mathbf{B}|$ [see Eq. (A1)] is a promising tool for decreasing the resonance frequency. In Fig. 5(c) we show the case $H = 20$ (when $\varepsilon_0 = 1$). The LSPR splits in this case into two branches, one of which [$\omega_{\text{res}-}$, see Eq. (29)] shifts by $\Delta\omega_1$ towards a lower frequency, while the other one [$\omega_{\text{res}+}$, see Eq. (28)] shifts in the opposite direction by $\Delta\omega_2$. After substitution of the used parameters, we get $\omega_{\text{res}-}/\omega_p \simeq 0.35$ and $\omega_{\text{res}+}/\omega_p \simeq 0.85$. Using both parameters $H = 20$ and $\varepsilon_0 = 10$ leads to a greater shift.

In Fig. 6 we show drawings similar to Fig. 5 but for a periodic array of *infinitely long* conducting *cylinders* (with radii $0.4a$) vs dimensionless frequency ω/ω_p. In Fig. 6(a) is shown the case of zero magnetic field $H = 0$, while $\varepsilon_0 = 1$. The LSPR appears at the frequency given by Eq. (34), where the depolarization factor n_x of the circular cylinder is 1/2. The other drawings are similar to Fig. 5. Note only that if the cylinders are not infinite but have finite length as for example is shown in Fig. 6(d) with length $l = 0.6a$, the LSPR appears at lower frequencies than predicted by Eq. (34). This is entirely due to the finite length of the cylinder, when the
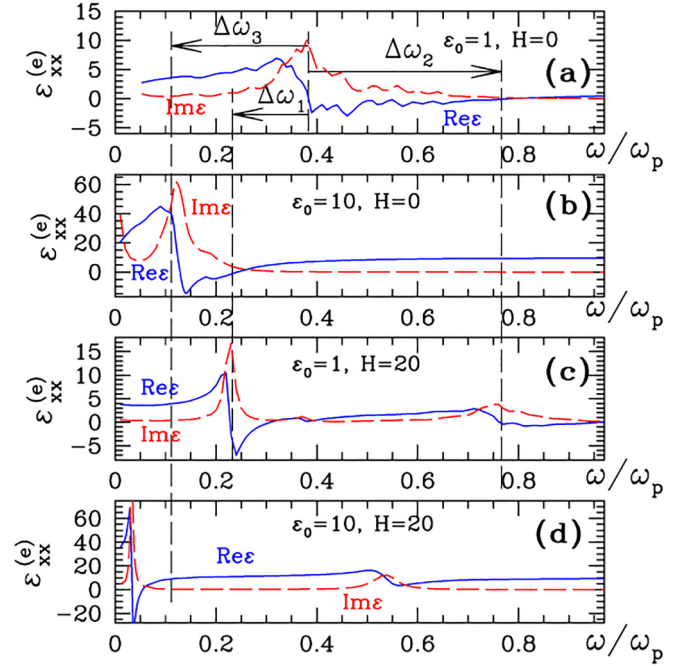

FIG. 5. Numerically calculated real (solid blue line) and imaginary (dashed red line) parts of $\varepsilon_{xx}^{(e)}$ of periodic array of conducting *spheres* vs dimensionless frequency ω/ω_p. **(a)** Magnetic field $H = 0$, while $\varepsilon_0 = 1$, [see Eq. (A1)]. The LSPR appears at the frequency $\omega_{\text{res}} = \omega_p \sqrt{\frac{(1-p_1)n}{\varepsilon_0}}$ [see Eq. (33)]. **(b)** Similar to Fig. (a) but for $\varepsilon_0 = 10$. **(c)** Similar to (a) but for $H = 20$ (while $\varepsilon_0 = 1$). The LSPR splits into the two branches (due to the applied field), one of which [$\omega_{\text{res}-}$, see Eq. (29)] shifts by $\Delta\omega_1$ to smaller values of ω/ω_p, while the second one [$\omega_{\text{res}+}$, see Eq. (28)] shifts in the opposite direction by $\Delta\omega_2$. **(d)** Similar to previous figures but for both parameters: $H = 20$ and $\varepsilon_0 = 10$. The LSPR splits into the two branches (due to applied magnetic field), one of which ($\omega_{\text{res}-}$) shifts by $\Delta\omega$ which is larger than in (c) due to parameter $\varepsilon_0 = 10$. In all figures the radii of spheres $R = 0.45a$, where a is the distance between sphere centers, $\omega_p \tau = 40$ [see Eq. (A1)], and $\varepsilon_{\text{host}} \equiv \varepsilon_2 = 1$. The vertical dashed lines are eye guides which indicate the appearance of the LSPR. The arrows indicate the shifts of the resonances.

behavior of the LSPR is qualitatively similar to the case of a sphere.

V. CONCLUSIONS

In the present paper we showed that using the LSPR it is possible to reach negative values of the permittivity ε in a wide range of frequencies ω by application of magnetic or electric fields. This can lead to attraction of like charged particles instead of repulsion and can be observed experimentally as destruction of electron-hole pairs and creation of hole-hole or electron-electron pairs similar to Cooper pairs. The latter can be used for new types of superconductivity in specially prepared metamaterials and in other interesting nontrivial applications. We conclude our paper with words from the article by Kirzhnits [6]: "Of course, the problem of the actual existence of structures with $\varepsilon(0, \mathbf{k}) < 0$ or of their artificial synthesis remains completely open, as yet. However,
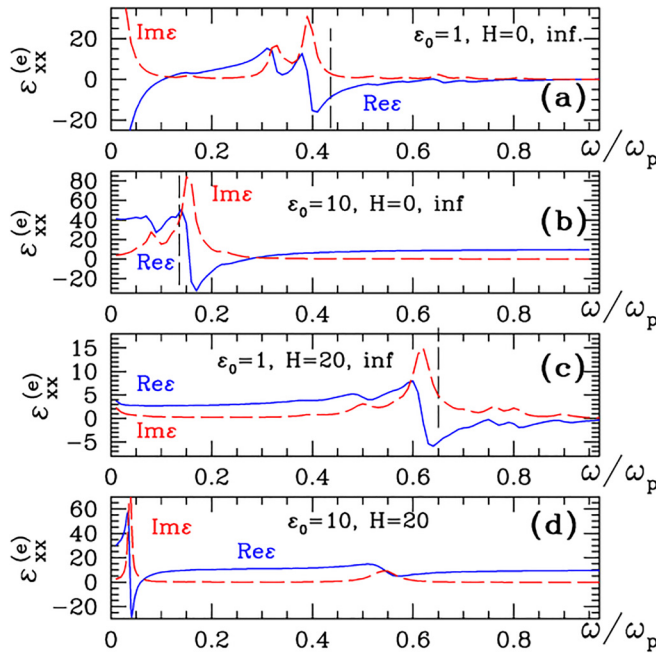
FIG. 6. Similar to Fig. 5, but for a periodic array of *infinitely long* conducting *cylinders* (**a**) Magnetic field $H = 0$, while $\varepsilon_0 = 1$ [see Eq. (A1)]. The LSPR appears at the frequency $\omega_{res}/\omega_p \simeq 0.43$ [see Eq. (34) with substitution n_x by $(1-p_1)n_x$], where the depolarization factor n_x of the circular cylinder is $1/2$ [see Eq. (32)]. (**b**) Similar to (a) but for $\varepsilon_0 = 10$. The LSPR [see Eq. (34)] shifts by $\sim\Delta\omega$ to smaller frequencies due to parameter $\varepsilon_0 = 10$. $\omega_{res}/\omega_p \simeq 0.2$ (**c**) Similar to (a) but for the case of applied magnetic field $H = 20$ (when $\varepsilon_0 = 1$). The LSPR shifts by $\Delta\omega$ to larger frequency. $\omega_{res}/\omega_p \simeq 0.66$ [see Eq. (34)]. (**d**) In (a)–(c) the cylinders are infinitely long, while in (d) the cylinders are of finite length $l = 0.6a$, where a is the distance between cylinder centers. $H = 20$. The LSPR appear at smaller frequencies. This is in contradiction to Eq. (34), since the cylinders have final length $l = 0.6a$ and, therefore, the behavior of the LSPR is qualitatively similar to behavior in the case of sphere. In all figures the radii of the cylinders $R = 0.45a$, $\omega_p\tau = 40$ [see Eq. (A1)], and $\varepsilon_{host} \equiv \varepsilon_2 = 1$. The vertical dashed lines indicate the values of the LSPR frequencies obtained from Eq. (34).

such a possibility cannot be excluded and it appears that the search for structures of this kind is an interesting and important problem of solid-state physics." The above words should be also correct for nucleus-nucleus pairing. However, the latter pairing due to a negative permittivity (in contrast with electron-electron pairing for which we have made detailed estimations) requires further intensive theoretical study.

APPENDIX A: DRUDE APPROXIMATION FOR THE PERMITTIVITY TENSOR

In the quasistatic regime the electric permittivity tensor of a metal, $\hat{\varepsilon}_M$, has the form [19,24–31]

$$\hat{\varepsilon}_M = \varepsilon_0 \cdot \hat{I} + i\frac{4\pi}{\omega}\hat{\sigma} = \varepsilon_0 \cdot \hat{I}$$

$$+ \frac{i\omega_p^2\tau}{\omega}\begin{pmatrix} \frac{1-i\omega\tau}{(1-i\omega\tau)^2+H^2} & \frac{-H}{(1-i\omega\tau)^2+H^2} & 0 \\ \frac{H}{(1-i\omega\tau)^2+H^2} & \frac{1-i\omega\tau}{(1-i\omega\tau)^2+H^2} & 0 \\ 0 & 0 & \frac{1}{1-i\omega\tau} \end{pmatrix}, \quad \text{(A1)}$$

where the conductivity tensor $\hat{\sigma}$ is taken in the free-electron Drude approximation (with the static magnetic field $\mathbf{B} \parallel z$), ε_0 is the scalar dielectric constant of the background ionic lattice and $\hat{I}$ is the unit tensor.

The magnetic field enters only through the Hall-to-Ohmic resistivity ratio $H \equiv \rho_H/\rho = \sigma_{yx}/\sigma_{xx} = \mu_e|\mathbf{B}| = \omega_c\tau$, where $\omega_c = eB/mc$ is the cyclotron frequency, τ is the conductivity relaxation time, $\omega_p = (4\pi e^2 N_0/m)^{1/2}$ is the plasma frequency, N_0 is the charge carrier concentration, m is the effective mass of the charge carriers, and μ_e is the electron Hall mobility [19,24–31].

APPENDIX B: COULOMB INTERACTION

In a medium, the Coulomb force of interaction changes (usually stated that it decreases) due to the phenomenon of polarization. Most explanations of this phenomenon presented in literature are only qualitative. Let us make here an elementary but quantitative consideration of this phenomenon and evaluate a characteristic of the medium which is called the dielectric constant or the permittivity ε directly from the Coulomb law. For simplicity, let us assume the medium is a cubic array of spheres as shown in Fig. 7. This medium is infinite in y and z directions, but bounded in the x direction (from $-L_1$ up to $+L_2$). A point charge q (shown as a black disk) is placed at $\mathbf{r} = (x, 0, 0)$, while a second point charge q_2 is placed at $\mathbf{r}_2 = (x_2, 0, 0) = (-x, 0, 0)$. These two point
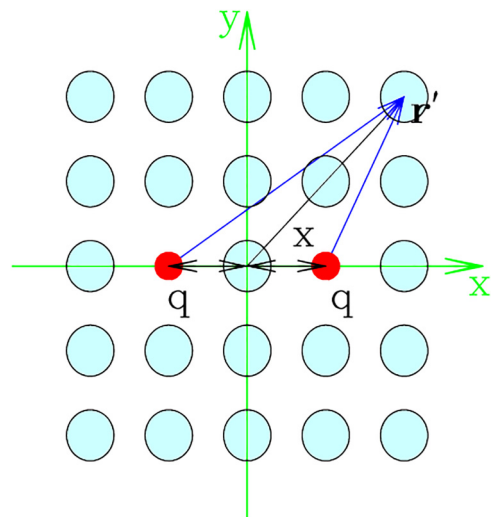

FIG. 7. Square lattice of dipoles. The z axis is perpendicular to the figure plane.

charges create an electric field and induce electric dipole moments **d** in all spheres (shown as blue circles) of the surrounding medium. In its turn, the electric field at **r**, which is created by the dipole **d** located at **r**′, is [53]

$$\mathbf{E} = \frac{3[(\mathbf{r}' - \mathbf{r}) \cdot \mathbf{d}](\mathbf{r}' - \mathbf{r})}{|\mathbf{r}' - \mathbf{r}|^5} - \frac{\mathbf{d}}{|\mathbf{r}' - \mathbf{r}|^3}. \tag{B1}$$

The force **F** of the Coulomb interaction of the point charge $q_1 = q$ with another point charge $q_2 = q$ and with all the dipoles **d** induced by them in the medium is

$$\mathbf{F} = \frac{q^2 \mathbf{e}_x}{(2x)^2} + q \sum_{\mathbf{r}'}' \left\{ \frac{3[(\mathbf{r}' - \mathbf{r}) \cdot \mathbf{d}](\mathbf{r}' - \mathbf{r})}{|\mathbf{r}' - \mathbf{r}|^5} - \frac{\mathbf{d}}{|\mathbf{r}' - \mathbf{r}|^3} \right\}, \tag{B2}$$

where $\mathbf{e}_x$ is the unit vector along the x axis. Here we sum over all dipoles with coordinates **r**′ excluding points **r**′ = **r** and **r**′ = $\mathbf{r}_2$. The induced dipole moment **d** is proportional to the applied external field

$$\mathbf{d} = \chi \mathbf{E}, \tag{B3}$$

where χ is the electric susceptibility of the medium. In general χ is a tensor, but for simplicity we consider it here as a scalar.

If we assume the crystal to be a lattice of spheres with permittivity ε_1 placed inside a medium with permittivity $\varepsilon_2 = 1$, then the dipole moment **d** of each sphere is determined by the expression [47]

$$\mathbf{d} = \chi \mathbf{E} = \frac{a^3}{3} \frac{\varepsilon_1 - 1}{1 + (\varepsilon_1 - 1)n} \mathbf{E}, \tag{B4}$$

where $n = 1/3$ is the depolarization factor of the sphere, a is the radius of the sphere, and **E** is the applied electric field. From Eq. (B4) it can be seen that the dipole moment **d**, as well as the susceptibility χ, can be both positive as well as negative (at resonance, see Sec. IV) depending on the parameters ε_1 and n. Physical intuition suggests that the permittivity ε of the entire sample [appearing in Eq. (2)] should be proportional to the dipole moment (B4), which implies that ε should also take negative values when Eq. (B4) is negative. However, as will be shown below, regardless of the magnitude and sign of the dipole moment **d**, their lattice sum (calculated using simple approximations and assumptions) is exactly zero. That is, this lattice sum does not contribute to the dielectric constant ε.

In our case **E** at **r**′ is created by the two point charges placed at **r** = $(x, 0, 0)$ and $\mathbf{r}_2 = (-x, 0, 0)$ and by dipoles $\mathbf{d}(\mathbf{r}'')$ placed at all other points **r**″. It can be expressed as

$$\mathbf{E}(\mathbf{r}') = \frac{q(\mathbf{r}' - \mathbf{r})}{|\mathbf{r}' - \mathbf{r}|^3} + \frac{q(\mathbf{r}' - \mathbf{r}_2)}{|\mathbf{r}' - \mathbf{r}_2|^3}$$
$$+ \sum_{\mathbf{r}''} \left\{ \frac{3[(\mathbf{r}'' - \mathbf{r}') \cdot \mathbf{d}(\mathbf{r}'')](\mathbf{r}'' - \mathbf{r}')}{|\mathbf{r}'' - \mathbf{r}'|^5} - \frac{\mathbf{d}(\mathbf{r}'')}{|\mathbf{r}'' - \mathbf{r}'|^3} \right\}. \tag{B5}$$

From the latter and Eq. (B3) we can find an expression for the dipole moment $\mathbf{d}(\mathbf{r}')$ at the point **r**′ as a solution of a system

of equations:

$$\mathbf{d}(\mathbf{r}') - \chi \sum_{\mathbf{r}''} \left\{ \frac{3[(\mathbf{r}'' - \mathbf{r}') \cdot \mathbf{d}(\mathbf{r}'')](\mathbf{r}'' - \mathbf{r}')}{|\mathbf{r}'' - \mathbf{r}'|^5} - \frac{\mathbf{d}(\mathbf{r}'')}{|\mathbf{r}'' - \mathbf{r}'|^3} \right\}$$
$$= q\chi \left[\frac{(\mathbf{r}' - \mathbf{r})}{|\mathbf{r}' - \mathbf{r}|^3} + \frac{(\mathbf{r}' - \mathbf{r}_2)}{|\mathbf{r}' - \mathbf{r}_2|^3} \right]. \tag{B6}$$

The off-diagonal terms of Eq. (B6) are of order $\sim 1/|\mathbf{r}|^3$, i.e., much less than the diagonal terms $\sim 1/|\mathbf{r}|^2$. Therefore, for simplicity of presentation we do not account for them in this Appendix in our further considerations (exact accounting of these off-diagonal terms would also drastically complicate the calculations). The influence of the off-diagonal terms we discuss in the Appendix C in the nearest-neighbors approximation. Hence, Eq. (B2) can be rewritten as

$$\mathbf{F} = \frac{q^2 \mathbf{e}_x}{(2x)^2} + q^2 \chi \sum_{\mathbf{r}'}' \left\{ \frac{3[(\mathbf{r}' - \mathbf{r}) \cdot (\mathbf{r}' - \mathbf{r})](\mathbf{r}' - \mathbf{r})}{|\mathbf{r}' - \mathbf{r}|^8} \right.$$
$$+ \frac{3[(\mathbf{r}' - \mathbf{r}) \cdot (\mathbf{r}' - \mathbf{r}_2)](\mathbf{r}' - \mathbf{r})}{|\mathbf{r}' - \mathbf{r}|^5 |\mathbf{r}' - \mathbf{r}_2|^3} - \frac{(\mathbf{r}' - \mathbf{r})}{|\mathbf{r}' - \mathbf{r}|^6}$$
$$\left. - \frac{(\mathbf{r}' - \mathbf{r}_2)}{|\mathbf{r}' - \mathbf{r}|^3 |\mathbf{r}' - \mathbf{r}_2|^3} \right\}. \tag{B7}$$

The sum of the first and third terms in braces leads to a simpler form:

$$\frac{3[(\mathbf{r}' - \mathbf{r}) \cdot (\mathbf{r}' - \mathbf{r})](\mathbf{r}' - \mathbf{r})}{|\mathbf{r}' - \mathbf{r}|^8} - \frac{(\mathbf{r}' - \mathbf{r})}{|\mathbf{r}' - \mathbf{r}|^6}$$
$$= \frac{3|\mathbf{r}' - \mathbf{r}|^2 (\mathbf{r}' - \mathbf{r})}{|\mathbf{r}' - \mathbf{r}|^8} - \frac{(\mathbf{r}' - \mathbf{r})}{|\mathbf{r}' - \mathbf{r}|^6} = \frac{2(\mathbf{r}' - \mathbf{r})}{|\mathbf{r}' - \mathbf{r}|^6}. \tag{B8}$$

The magnitude of the force (B7) can be written as

$$|\mathbf{F}| = \frac{q^2}{(2x)^2} \left| \left[1 + (2x)^2 \chi \sum_{\mathbf{r}'} \left\{ \frac{2(\mathbf{r}' - \mathbf{r})}{|\mathbf{r}' - \mathbf{r}|^6} \right. \right. \right.$$
$$+ \frac{3[(\mathbf{r}' - \mathbf{r}) \cdot (\mathbf{r}' - \mathbf{r}_2)](\mathbf{r}' - \mathbf{r})}{|\mathbf{r}' - \mathbf{r}|^5 |\mathbf{r}' - \mathbf{r}_2|^3}$$
$$\left. \left. \left. - \frac{(\mathbf{r}' - \mathbf{r}_2)}{|\mathbf{r}' - \mathbf{r}|^3 |\mathbf{r}' - \mathbf{r}_2|^3} \right\} \right] \right|. \tag{B9}$$

We should check whether the expression in the square brackets is the inverse permittivity $1/\varepsilon$. The first sum in Eq. (B9) simplifies to the form

$$\sum_{\mathbf{r}'} \frac{2(\mathbf{r}' - \mathbf{r})}{|\mathbf{r}' - \mathbf{r}|^6} = \sum_{\mathbf{r}'} \frac{2(x' - x)\mathbf{e}_x + 2y'\mathbf{e}_y + 2z'\mathbf{e}_z}{[(x' - x)^2 + y'^2 + z'^2]^3}$$
$$= \mathbf{e}_x \sum_{\mathbf{r}'} \frac{2(x' - x)}{[(x' - x)^2 + y'^2 + z'^2]^3}, \tag{B10}$$

since the sum along $\mathbf{e}_y$ and $\mathbf{e}_z$ axes cancel due to symmetry of the cubic lattice ($\mathbf{e}_y$, and $\mathbf{e}_z$ are the unit vectors along Cartesian y and z axes, respectively). Let us consider the slab of thickness $2L$ (from $x' = -L$ up to $x' = +L$, where $L \to \infty$). The sizes in y and z directions are infinite (see Fig. 7). The sum (B10) should be zero. This can be seen if we shift the origin of the system of coordinates to the point x (i.e., when $x' - x \to x'$). This also can be verified by direct evaluation of the sum (B10) where for simplicity we evaluate the

above lattice sums in continuous approximation. Integration in y', z' plane is convenient to perform in polar coordinates: $0 \leqslant \varphi \leqslant 2\pi$ and $0 \leqslant \rho \leqslant \infty$. The area of integration along the x' axis we define by theta function $\theta(x')$. Sum (B10), therefore, can be rewritten in continuous approximation (in limit $L \to \infty$) as

$$4\pi \int \theta(x')(x' - x)dx' \int_0^\infty \frac{\rho d\rho}{[(x' - x)^2 + \rho^2]^3} = \pi \int_{-L}^{+L} \frac{(x' - x)dx'}{(x' - x)^2} = \pi \ln\left(\frac{L - x}{L + x}\right)^2 \to 0. \tag{B11}$$

The sum of the second and the third terms in the braces of Eq. (B9) can be simplified to the form

$$\sum_{\mathbf{r}'} \left\{ \frac{3[(\mathbf{r}' - \mathbf{r}) \cdot (\mathbf{r}' - \mathbf{r}_2)](\mathbf{r}' - \mathbf{r})}{|\mathbf{r}' - \mathbf{r}|^5 |\mathbf{r}' - \mathbf{r}_2|^3} - \frac{(\mathbf{r}' - \mathbf{r}_2)}{|\mathbf{r}' - \mathbf{r}|^3 |\mathbf{r}' - \mathbf{r}_2|^3} \right\}$$

$$= \mathbf{e}_x \sum_{x',y',z'} \left\{ \frac{1}{[(x' - x)^2 + y'^2 + z'^2]^{3/2}[(x' + x)^2 + y'^2 + z'^2]^{3/2}} \left[\frac{3(x' - x)^2(x' + x) + 3(y'^2 + z'^2)(x' - x)}{[(x' - x)^2 + y'^2 + z'^2]} - (x' + x) \right] \right\}$$

$$= \mathbf{e}_x \sum_{x',y',z'} \frac{2[(x' - x)^2(x' + x) + (y'^2 + z'^2)(x' - 2x)]}{[(x' - x)^2 + y'^2 + z'^2]^{5/2}[(x' + x)^2 + y'^2 + z'^2]^{3/2}}$$

$$= \mathbf{e}_x \sum_{x',y',z'} \left\{ \frac{2(x' + x)}{[(x' - x)^2 + y'^2 + z'^2]^{3/2}[(x' + x)^2 + y'^2 + z'^2]^{3/2}} - \frac{6x(y'^2 + z'^2)}{[(x' - x)^2 + y'^2 + z'^2]^{5/2}[(x' + x)^2 + y'^2 + z'^2]^{3/2}} \right\}. \tag{B12}$$

As in Eq. (B10), the sum along $\mathbf{e}_y$ and $\mathbf{e}_z$ axes cancel due to symmetry of the cubic lattice. Similarly to Eq. (B11), we can rewrite the lattice sums (B12) in continuous approximation (we also took into account that $x_2 = -x$):

$$4\pi \left\{ \int \theta(x')(x' + x)dx' \int_0^\infty \frac{\rho d\rho}{[(x' - x)^2 + \rho^2]^{3/2}[(x' + x)^2 + \rho^2]^{3/2}} \right.$$

$$\left. - 3x \int \theta(x')dx' \int_0^\infty \frac{\rho^3 d\rho}{[(x' - x)^2 + \rho^2]^{5/2}[(x' + x)^2 + \rho^2]^{3/2}} \right\}. \tag{B13}$$

The first integral in Eq. (B13) over $d\rho$ is

$$-\frac{\rho^2 + x'^2 + x^2}{8x'^2 x^2 \sqrt{\rho^2 + (x' - x)^2} \sqrt{\rho^2 + (x' + x)^2}} \Bigg|_0^\infty = -\frac{1}{8x'^2 x^2} + \frac{x'^2 + x^2}{8x'^2 x^2 |x' - x||x' + x|}. \tag{B14}$$

The second integral in Eq. (B13) over $d\rho$ is

$$-\frac{(x'^2 - x^2)^2(x'^2 - x'x + x^2) + \rho^4(x'^2 + x'x + x^2) + 2\rho^2(x'^4 + x'^2 x^2 + x^4)}{24x'^3 x^3 [\rho^2 + (x' - x)^2]^{3/2} \sqrt{\rho^2 + (x' + x)^2}} \Bigg|_0^\infty$$

$$= -\frac{(x'^2 + x'x + x^2)}{24x'^3 x^3} + \frac{(x'^2 - x^2)^2(x'^2 - x'x + x^2)}{24x'^3 x^3 |x' - x|^3 |x' + x|}. \tag{B15}$$

After substitution of Eq. (B15) into the second integral of Eq. (B13) we get the following expression:

$$\frac{2\pi}{(2x)^2} \left[\int \theta(x') \frac{(x'^2 + x'x + x^2)dx'}{x'^3} - \int \theta(x') \frac{(x'^2 - x^2)^2(x'^2 - x'x + x^2)dx'}{x'^3 |x' - x|^3 |x' + x|} \right]. \tag{B16}$$

The second integral in Eq. (B16) can be transformed to the form

$$\int \theta(x') \frac{(x' + x)(x'^2 + x^2)dx'}{x'^2 |x' - x||x' + x|} + x^2 \int \theta(x') \frac{(x' + x)(x - x')dx'}{x'^3 |x' - x||x' + x|}. \tag{B17}$$

Substituting Eqs. (B14), (B16), and (B17) into Eq. (B13) we get

$$\frac{2\pi x^2}{(2x)^2} \left[\int \theta(x') \frac{dx'}{x'^3} - \int \theta(x') \frac{(x' + x)(x - x')dx'}{x'^3 |x' - x||x' + x|} \right]. \tag{B18}$$

The first integral in Eq. (B18) with symmetric limits is zero as an integral of an odd function. The second integral in the last expression should be evaluated carefully since in the denominator are absolute values. This integral is zero in symmetric

limits:

$$\int \theta(x') \frac{(x'+x)(x-x')dx'}{x'^3|x'-x||x'+x|}$$

$$= \int_{-L}^{-x} \frac{(x'+x)(x-x')dx'}{x'^3(x'-x)(x'+x)} - \int_{-x}^{x} \frac{(x'+x)(x-x')dx'}{x'^3(x'-x)(x'+x)}$$

$$+ \int_{x}^{L} \frac{(x'+x)(x-x')dx'}{x'^3(x'-x)(x'+x)} = 0. \tag{B19}$$

This way, we found that the dipole lattice in Eq. (B9) is zero, i.e., the polarization of the crystal does not contribute to the permittivity within the framework of the considered classical model and, therefore, $\varepsilon = 1$. This is partially reminiscent of the Lorentz' result [17,54] and shows that the field due to the nearby atoms in a simple cubic lattice vanishes at any lattice site. Our result appears either because of the above dipole approximation (which is probably not enough) or due to some other simplifications the main of which is neglecting of off-diagonal terms in Eq. (B4). It is also possible that zeroing out the lattice sum has a deeper reason: It is interesting to compare this with the phenomenon of magnetization. The appearance of magnetic permeability $\mu > 1$ (i.e., magnetization) of samples was explained for a long time as the result of the summation of the molecular circular currents. However, the circular currents inside the samples as well (as the dipole moments in our cases) are mutually compensated. Only those currents (and molecular dipole moments in our case) remain uncompensated which are located near the side sample surfaces. However, in respect to magnetization it was shown by the Bohr-Van Leeuwen theorem that this explanation is not correct and the magnetism in solids is solely a quantum mechanical effect and means that classical physics cannot account for paramagnetism, diamagnetism, ferromagnetism, etc. Probably, the result obtained in this chapter by simple integration, suggests that the permittivity, similarly to magnetization, cannot be explained within the framework of classical theory.

Note for comparison, that in Ref. [41] within studies of excitons in the framework of quantum mechanics, the following expression was obtained for the permittivity

$$\varepsilon = \frac{1}{1 - \sum_i \frac{\gamma_i^2}{2\pi \Delta \tilde{E}_i}}, \tag{B20}$$

where the summation is over all ith excited exciton states, $\gamma = 4\pi e|\vec{\mu}|/\sqrt{V_0}$, $\vec{\mu}$ is dipole moment, V_0 is the volume of the crystal unit cell, $\Delta \tilde{E} = \hbar\Omega_\parallel(0)$ (in definitions of Authors) [see text after Eq. (4.18) in Ref. [41]]. Since the permittivity ε
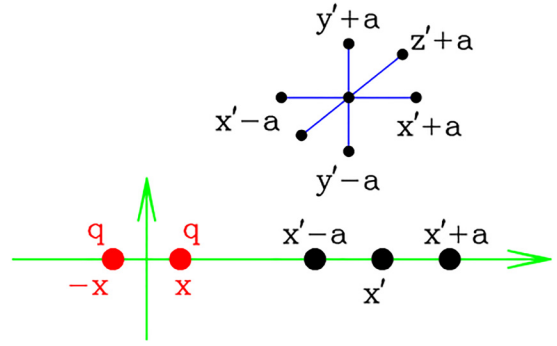

FIG. 8. Sketch for accounting the off-diagonal terms of Eq. (B6) in nearest-neighbors approximation.

is usually greater or equal to one, the sum in the denominator of Eq. (B20) must be positive and smaller than one. It can be assumed that when this sum is greater than 1, then the permittivity will become negative. However, whether this is possible in the case of exciton systems requires further analyses. It is also required to find out whether the expression similar to Eq. (B20) is valid for other (nonexcitonic) quantum systems. Anyway, in the case of plasmons, the negative permittivity is observed both in theory and in experiment.

Despite the result of calculation of the lattice sum contradicts to our expectations (i.e., the sum is zero and is not proportional to **d**), we provided here a detailed presentation of our calculations in order to attract the attention of scientists to the nontriviality of this problem.

APPENDIX C: ACCOUNTING OF THE OFF-DIAGONAL TERMS IN NEAREST-NEIGHBOR APPROXIMATION

Exact accounting of the off-diagonal terms in Eq. (B6) is a complicated problem. In this Appendix we justify qualitatively that accounting of these terms does not change the above obtained result. Let us consider this problem in the nearest-neighbor approximation.

1. First way

For convenience, let us write out Eq. (B6) in expanded form for the points (for simplicity of presentation we consider the 2D case) $\mathbf{r}' = (x', y')$ and $\mathbf{r}'' = (x'+a, y')$, $(x'-a, y')$, $(x', y'+a)$, $(x', y'-a)$ [where $(\pm a, 0)$ and $(0, \pm a)$, are the distances between two neighbors in two x and y directions, see Fig. 8]:

$$d_x(x', y') - \chi \frac{3[(x'+a-x')d_x(x'+a, y') + (y'-y')d_y(x'+a, y')](x'+a-x')}{[(x'+a-x')^2 + (y'-y')^2]^{5/2}} + \chi \frac{d_x(x'+a, y')}{[(x'+a-x')^2 + (y'-y')^2]^{3/2}}$$

$$- \chi \frac{3[(x'-a-x')d_x(x'-a, y') + (y'-y')d_y(x'-a, y')](x'-a-x')}{[(x'-a-x')^2 + (y'-y')^2]^{5/2}} + \chi \frac{d_x(x'-a, y')}{[(x'-a-x')^2 + (y'-y')^2]^{3/2}}$$

$$- \chi \frac{3[\dots](x'-x')}{[\dots]^{5/2}} + \chi \frac{d_x(x', y'+a)}{[\dots]^{3/2}} - \chi \frac{3[\dots](x'-x')}{[\dots]^{5/2}} + \chi \frac{d_x(x', y'-a)}{[\dots]^{3/2}}$$

$$= q\chi \left[\frac{x'-x)}{|\mathbf{r}'-\mathbf{r}|^3} + \frac{(x'+x)}{|\mathbf{r}'-\mathbf{r}_2|^3} \right]. \tag{C1}$$

Expanding the dipole moment $d(x)$ in a Taylor series $d_x(x' \pm a, y') \simeq d_x(x', y') \pm \frac{\partial d_x}{\partial x} a$ and $d_x(x', y' \pm a) \simeq d_x(x', y') \pm \frac{\partial d_x}{\partial y} a$, we find that

$$d_x(x, y) = \frac{q\chi}{1 - \frac{2\chi}{a^3}} \left[\frac{x' - x}{|\mathbf{r}' - \mathbf{r}|^3} + \frac{x' + x}{|\mathbf{r}' - \mathbf{r}_2|^3} \right]. \quad (C2)$$

That is, the accounting of the diagonal terms in Eqs. (B6) leads only to renormalization of the coefficient χ. The lattice sums with these terms were already calculated in Appendix B and gave a vanishing result.

2. Second way

Let us write out Eq. (B6) in the 1D case

$$d_x(x') - \frac{3\chi}{a^3} [d_x(x' + a) + d_x(x' - a)] + \frac{\chi}{a^3}$$

$$\times [d_x(x' + a) + d_x(x' - a)] = q\chi \left[\frac{1}{(x' - x)^2} + \frac{1}{(x' + x)^2} \right]. \quad (C3)$$

This can be rewritten as

$$d_x(x') - \frac{2\chi}{a} \frac{[d_x(x' + a) - 2d_x(x') + d_x(x' - a)]}{a^2}$$

$$- \frac{4\chi}{a^3} d_x(x') = q\chi \left[\frac{1}{(x' - x)^2} + \frac{1}{(x' + x)^2} \right]. \quad (C4)$$

The terms in the left-hand side can be understood as the second derivative $d^2 d_x/dx^2$ of the dipole moment, written in terms of finite differences. Therefore, we have

$$\frac{d^2 d_x(x')}{dx^2} + \kappa_0^2 d_x(x') = -\frac{aq}{2} \left[\frac{1}{(x' - x)^2} + \frac{1}{(x' + x)^2} \right], \quad (C5)$$

where $\kappa_0^2 = \frac{4\chi/a^3 - 1}{2\chi/a}$. The solution of this equation is

$$d_x(x') = C_1 e^{i\kappa_0 x} + C_2 e^{-i\kappa_0 x} + C_3 \left[\frac{1}{(x' - x)^2} + \frac{1}{(x' + x)^2} \right]. \quad (C6)$$

The third part of this solution (C6) with coefficient C_3 is not important since it was already included in the lattice sum and evaluated in Appendix B. The other part of the solution (C6) with coefficients C_1 and C_2 are decaying or oscillating (depending on the sign of κ_0^2) terms. Therefore, we can look for the solution of Eq. (B6) in the form $d \sim e^{i\kappa_0 \cdot x}$ and write $d_i(\mathbf{r}' \pm \mathbf{a}_i) \simeq d_i(\mathbf{r}') \exp(\pm i\kappa_{0i} a_i)$, where $i = x, y, z$. Then from Eq. (B6) it follows (if $a_x = a_y = a_z$):

$$\left[1 - \frac{2\chi}{a^3} (2\cos\kappa_{0x}a - \cos\kappa_{0y}a - \cos\kappa_{0z}a) \right] d_x(x', y', z') =$$

$$= \chi q \left[\frac{(\mathbf{r}' - \mathbf{r})}{|\mathbf{r}' - \mathbf{r}|^3} + \frac{(\mathbf{r}' - \mathbf{r}_2)}{|\mathbf{r}' - \mathbf{r}_2|^3} \right]_x. \quad (C7)$$

That is, the accounting of the diagonal terms in Eqs. (B6) again leads only to renormalization (if $\kappa_{0x} \neq \kappa_{0y} \neq \kappa_{0z}$) of the coefficient χ and the results of the lattice summation should be the same as in Appendix B. In our opinion, despite the approximate nature of the calculations carried out in the previous, and especially the present Appendix, the obtained result reflects the symmetry of the problem and has a deep physical meaning.

[1] V. G. Veselago, The electrodynamics of substances with simultaneously negative values of ϵ and μ, Sov. Phys. Usp. **10**, 509 (1968); Usp. Fiz. Nauk **92**, 517 (1967).

[2] J. B. Pendry, Negative refraction makes a perfect lens, Phys. Rev. Lett. **85**, 3966 (2000).

[3] T. W. Ebbesen, H. J. Lezec, H. F. Ghaemi, T. Thio, and P. A. Wolff, Extraordinary optical transmission through subwavelength hole arrays, Nature (London) **391**, 667 (1998).

[4] I. Karakasoglu and S. Fan, Controlling the electrostatic coulomb interaction using metamaterials, Phys. Rev. B **93**, 075433 (2016).

[5] V. L. Ginzburg, Superconductivity: The day before yesterday–yesterday–today–tomorrow, Phys. Usp. **43**, 573 (2000).

[6] D. A. Kirzhnits, Are the Kramers-Kronig relations for the dielectric permittivity always valid? Sov. Phys. Usp. **19**, 530 (1976).

[7] B. Friess, Y. Peng, B. Rosenow, F. von Oppen, V. Umansky, K. von Klitzing, and J. H. Smet, Negative permittivity in bubble and stripe phases, Nat. Phys. **13**, 1124 (2017); Negative permittivity attests to local attractive interactions in bubble and stripe phases, arXiv:1608.05210.

[8] C. W. Chu, F. Chen, J. Shulman, S. Tsui, Y. Y. Xue, W. Wen, and P. Sheng, A negative dielectric constant in nano-particle

materials under an electric field at very low frequencies, Proc. SPIE **5932**, 59320X (2005).

[9] V. N. Smolyaninova, C. Jensen, W. Zimmerman, J. C. Prestigiacomo, M. S. Osofsky, H. Kim, N. Bassim, Z. Xing, M. M. Qazilbash, and I. I. Smolyaninov, Enhanced superconductivity in aluminum-based hyperbolic metamaterials, Sci. Rep. **6**, 34140 (2016).

[10] A. A. Rangelov and N. Karchev, Coulomb interaction revised in the presence of material with negative permittivity, arXiv:0910.5307.

[11] V. B. Bobrov, S. A. Trigger, G. J. F. van Heijst, and P. P. J. M. Schram, Kramers-Kronig relations for the dielectric function and the static conductivity of Coulomb systems, Europhys. Lett. **90**, 10003 (2010).

[12] A. Hamo, A. Benyamini, I. Shapir, I. Khivrich, J. Waissman, K. Kaasbjerg, Y. Oreg, F. von Oppen, and S. Ilani, Electron attraction mediated by Coulomb repulsion, Nature (London) **535**, 395 (2016).

[13] F. Castles, J. A. J. Fells, D. Isakov, S. M. Morris, A. A. R. Watt, and P. S. Grant, Active metamaterials with negative static electric susceptibility, Adv. Mater. **32**, 1904863 (2020).

[14] X. Li, C. Li, X. Gao, and D. Huang, Like-charge attraction between two identical dielectric spheres in a uniform electric

field: A theoretical study via a multiple-image method and an effective-dipole approach, J. Mater. Chem. A **12**, 6896 (2024).

[15] A. P. dos Santos and Y. Levin, Like-charge attraction between metal nanoparticles in a 1:1 electrolyte solution, Phys. Rev. Lett. **122**, 248005 (2019).

[16] M. Holten, L. Bayha, K. Subramanian, S. Brandstetter, C. Heintze, P. Lunt, P. M. Preiss, and S. Jochim, Observation of Cooper pairs in a mesoscopic two-dimensional Fermi gas, Nature (London) **606**, 287 (2022).

[17] J. D. Jackson, *Classical Eectrodynamics* (Wiley, New York, 1962).

[18] D. J. Bergman and Y. M. Strelniker, Magneto-transport in conducting composite films with a disordered columnar microstructure and an in-plane magnetic field, Phys. Rev. B **60**, 13016 (1999).

[19] Y. M. Strelniker, D. Stroud, and A. O. Voznesenskaya, Control of extraordinary light transmission through perforated metal films using liquid crystals, Eur. Phys. J. B **52**, 1 (2006).

[20] H. C. Baker and R. L. Singleton, Jr., Non-Hermitian quantum dynamics, Phys. Rev. A **42**, 10 (1990).

[21] C. M. Bender, D. C. Brody, and H. F. Jones, Complex extension of quantum mechanics, Phys. Rev. Lett. **89**, 270401 (2002).

[22] J. P. Sun, G. I. Haddad, P. Mazumder, and J. N. Schulman, Resonant tunneling diodes: Models and properties, Proc. IEEE **86**, 641 (1998).

[23] L. D. Landau and E. M. Lifshitz, *Mechanics: Course of Theoretical Physics* (Butterworth-Heinemann, Oxford, 1976), Vol. 1.

[24] D. J. Bergman and Y. M. Strelniker, Anisotropic ac electrical permittivity of a periodic metal-dielectric composite film in a strong magnetic field, Phys. Rev. Lett. **80**, 857 (1998).

[25] Y. M. Strelniker and D. J. Bergman, Magneto-optical properties of metal-dielectric composites with a periodic microstructure, Eur. Phys. J. AP **7**, 19 (1999).

[26] Y. M. Strelniker and D. J. Bergman, Optical transmission through metal films with a subwavelength hole array in the presence of a magnetic field, Phys. Rev. B **59**, R12763 (1999).

[27] Y. M. Strelniker, Theory of optical transmission through elliptical nanohole arrays, Phys. Rev. B **76**, 085409 (2007).

[28] Y. Fleger, M. Rosenbluh, Y. M. Strelniker, D. J. Bergman, and A. N. Lagarkov, Controlling the optical spectra of gold nano-islands by changing the aspect ratio and the inter-island distance: Theory and experiment, Eur. Phys. J. B **81**, 85 (2011).

[29] Y. M. Strelniker and D. J. Bergman, Strong angular magneto-induced anisotropy of Voigt effect in metal-dielectric metamaterials with periodic nanostructures, Phys. Rev. B **89**, 125312 (2014).

[30] Y. M. Strelniker and D. J. Bergman, Surface versus localized plasmons in an assembly of metal-dielectric parallel flat slabs in the presence of an in-plane magnetic field, Phys. Rev. B **102**, 035302 (2020).

[31] Y. M. Strelniker and D. J. Bergman, Transmittance and transparency of subwavelength-perforated conducting films in the presence of a magnetic field, Phys. Rev. B **77**, 205113 (2008).

[32] M. Tornow, D. Weiss, K. von Klitzing, K. Eberl, D. J. Bergman, and Y. M. Strelniker, Anisotropic magnetoresistance of a classical antidot array, Phys. Rev. Lett. **77**, 147 (1996).

[33] G. J. Strijkers, F. Y. Yang, D. H. Reich, C. L. Chien, P. C. Searson, Y. M. Strelniker, and D. J. Bergman, Magnetoresistance anisotropy of a Bi antidot array, IEEE Trans. Magn. **37**, 2067 (2001).

[34] Y. M. Strelniker and D. J. Bergman, Gate-tuning of the surface plasmons and their optical properties, Proc. SPIE **12197**, 1219706 (2022).

[35] R. S. Knox, *Theory of Excitons* (Academic, New York, 1963).

[36] G. H. Wannier, The structure of electronic excitation levels in insulating crystals, Phys. Rev. **52**, 191 (1937).

[37] N. F. Mott, Conduction in polar crystals. II. The conduction band and ultra-violet absorption of alkali-halide crystals, Trans. Faraday Soc. **34**, 500 (1938).

[38] G. Dresselhaus, Effective mass approximation for excitons, J. Phys. Chem. Solids **1**, 14 (1956).

[39] V. N. Piskovoi, E. F. Venger, and Y. M. Strelniker, Theory of polaritons in bounded spatially dispersive media, Phys. Rev. B **66**, 115402 (2002).

[40] Y. M. Strelniker, Theory of inelastic low-energy electron scattering with generation of surface and bulk excitons in molecular crystals, Phys. Stat. Sol. B **149**, 603 (1988).

[41] H. Haken and W. Schottky, Die behandlung des exzitons nach der vielelektronentheorie, Z. Phys. Chem. Neue Folge **16**, 218 (1958).

[42] H. Haken, Die theorie des exzitons im festen körper, Fortschr. Phys. **6**, 271 (1958).

[43] V. L. Ginzburg and V. V. Kelle, Surface excitons of electron-hole type and collective phenomena associated with them, JETP Lett. **17**, 306 (1973) [ZhETF Pis. Red. **17**, 428 (1973)].

[44] L. V. Keldysh, Exciton in semiconductor-dielectric nanostructures, Phys. Stat. Sol. (a) **164**, 3 (1997).

[45] L. V. Keldysh, Sov. Phys. J. Exper. Theor. Phys. Lett. **29**, 716 (1979).

[46] E. V. Shornikova, D. R. Yakovlev, N. A. Gippius, G. Qiang, B. Dubertret, A. H. Khan, A. D. Giacomo, I. Moreels, and M. Bayer, Exciton binding energy in CdSe nanoplatets measured by one- and two-photon absorption, Nano Lett. **21**, 10525 (2021).

[47] L. D. Landau, L. P. Pitaevskii, and E. M. Lifshitz, *Electrodynamics of Continuous Media* (Pergamon, Oxford, 1984).

[48] L. D. Landau and L. M. Lifshitz, *Quantum Mechanics: Non-Relativistic Theory*, 3rd ed. (Butterworth, Heinemann, Oxford, 2003).

[49] V. B. Berestetskii, L. P. Pitaevskii, and E. M. Lifshitz, *Quantum Electrodynamics: Course of Theoretical Physics*, Vol. 4 (Pergamon, 1982).

[50] D. J. Bergman, Eigenstates of Maxwell's equations in multiconstituent microstructures, Phys. Rev. A **105**, 062213 (2022).

[51] G. Dresselhaus, A. F. Kip, and C. Kittel, Cyclotron resonance of electrons and holes in silicon and germanium crystals, Phys. Rev. **98**, 368 (1955).

[52] G. Dresselhaus, A. F. Kip, and C. Kittel, Plasma resonance in crystals: Observations and theory, Phys. Rev. **100**, 618 (1955).

[53] L. D. Landau and E. M. Lifshitz, *The Classical Theory of Field*, 4th revised English edition (Pergamon, Oxford, 1987).

[54] H. A. Lorentz, *The Theory of Electrons: And Its Applications to the Phenomena of Light and Radiant Heat*, 2nd ed. (Dover, New York, 1952), p. 158.